*Journal of the European Ceramic Society* **10** (1992) 65–74

# Stoichiometry and Crystal Structure of X-phase Sialon

C. C. Anya & A. Hendry*

Department of Metallurgy & Engineering Materials, University of Strathclyde, Glasgow, UK, G1 1XN

(Received 22 October 1991; revised version received and accepted 2 December 1991)

***Abstract***

*Stable x-phase sialon can be produced through simultaneous carbothermal reduction and nitridation of kaolinite or kaolinite plus <5 wt (11·7 mol) % α-alumina at 1500°C. The three different formulae suggested in the literature for x-phase sialon and their equivalent percent of aluminium (eq% Al) are reviewed.*

*Using the crystalline phases from X-ray diffraction (XRD) patterns, it is argued that the monophasic domain of x-phase existence is a narrow region which extends from 42·9 to 49·6 eq% Al. This region extends upwards towards the $SiO_2$–$Al_2O_3$ line in the $Si_3N_4$–$AlN$–$SiO_2$–$Al_2O_3$ phase equilibrium diagram. Consequently, $Si_{12}Al_{18}O_{39}N_8$ is favoured to be the closest formula.*

*The interplanar distances observed from the XRD pattern were used to determine the lattice parameters of the phase. X-phase is present in its low form, with a triclinic crystal structure of $a = 9{\cdot}68$ Å, $b = 8{\cdot}55$ Å, $c = 11{\cdot}21$ Å; $\alpha = 91{\cdot}4°$, $\beta = 124{\cdot}4°$ and $\gamma = 99{\cdot}2°$ from the XRD pattern. However, in electron diffraction (ED), patterns are indexed as an orthorhombic structure of $a = 9{\cdot}66$ Å, $b = 2{\cdot}84$ Å and $c = 11{\cdot}17$ Å.*

*Stabiles x-phasiges Sialon kann durch gleichzeitige karbothermische Reduktion und Nitrierung von Kaolinit oder von Kaolinit mit weniger als 5 Gew.% (11·7 Mol%) α-Aluminiumoxid-Zusatz bei 1500°C hergestellt werden. Die drei verschiedenen Formeln für x-phasiges Sialon und die entsprechenden Aluminium-Gehalte in Äquivalent-Prozent (Äq.% Al), welche im Schrifttum vorgeschlagen werden, wurden überprüft.*

*Aus der Auswertung der Röntgenbeugungsdiagramme der kristallinen Phasen wird geschlossen, daß das Einphasengebiet der x-Phase ein enger Bereich ist, der sich von 42·9 bis zu 49·6 Äq.% Al erstreckt. Dieser Bereich dehnt sich bis zur $SiO_2$–$Al_2O_3$–Linie im Phasen-Gleichgewichtsdiagramm des Systems $Si_3N_4$–$AlN$–$SiO_2$–$Al_2O_3$ aus. Demnach scheint, $Si_{12}Al_{18}O_{39}N_8$ die am nächsten liegende Formel zu sein.*

*Zur Bestimmung der Gitterparameter wurden die Netzebenenabstände, die aus den Röntgenbeugungsdiagrammen erhalten wurden, ausgewertet. In ihrer einfachen Form besitzt die x-Phase eine trikline Kristallstruktur mit $a = 9{\cdot}68$ Å, $b = 8{\cdot}55$ Å und $c = 11{\cdot}21$ Å; aus den Röntgenbeugungsdiagrammen folgt des weiteren: $\alpha = 91{\cdot}4°$, $\beta = 124{\cdot}4°$ und $\gamma = 99{\cdot}2°$. Aus Elekronenbeugungsexperimenten jedoch konnten Begungsdiagramme mit orthorhombischer Struktur indiziert werden: $a = 9{\cdot}66$ Å, $b = 2{\cdot}84$ Å und $c = 11{\cdot}17$ Å.*

*Une phase Ẋ stable de sialon peut être produite par réduction carbothermique et nitruration simultanées de kaolinite ou de kaolinite avec moins de 5% en poids (11·7% en mol) d'alumine α à 1500°C. Les trois différentes formules suggérées par la littérature pour la phase Ẋ de sialon et leur équivalent en pourcent d'aluminium (eq% Al) sont passés en revue.*

*En utilisant les clichés de diffractions de rayon X des phases cristallines, l'existence d'un domaine monophasique de la phase Ẋ sous forme d'une région étroite qui s'étend de 42·9 à 49·6 eq% Al est montré. Cette région s'étend vers le haut à travers la ligne $SiO_2$–$Al_2O_3$ dans le diagramme de phase $Si_3N_4$–$AlN$–$SiO_2$–$Al_2O_3$. En conséquence la formule retenue comme étant la plus proche est $Si_{12}Al_{18}O_{39}N_8$.*

*Les distances interplans observées à partir des clichés de diffraction sont utilisées pour déterminer les paramètres de réseau de la phase. La phase Ẋ est présente sous sa forme basse avec une structure*

* To whom correspondence should be addressed.

*cristalline triclinique $a = 9{\cdot}68$ Å, $b = 8{\cdot}55$ Å, $c = 11{\cdot}21$ Å; $\alpha = 91{\cdot}4°$, $\beta = 124{\cdot}4°$ et $\gamma = 99{\cdot}2°$. Cependant par diffraction électronique (ED) une structure orthorombique $a = 9{\cdot}66$ Å, $b = 2{\cdot}84$ Å, $c = 11{\cdot}17$ Å a été caractérisée à partir des clichés.*

## 1 Introduction

Until now, reports[1-4] on the formation of X-phase sialon have almost exclusively been from reaction-sintered powders in the $Si_3N_4$–AlN–$SiO_2$–$Al_2O_3$ system, at temperatures of 1700 to 1780°C for different holding times. The phase was reported[4] to be a point composition and has been represented[3,5] as such, with equivalent percent aluminium (eq% Al—see the footnote to Fig. 1) of about 53%[3] and 60%[5], respectively. However, Jack,[6] from studies on samples heated between 1550 and 2000°C, represented the phase as an extended region, with eq% Al varying from 53 to 58% (Fig. 1).

As the graphical representations vary so also do the stoichiometric formulae that have been suggested to represent the phase. The first formula is $Si_3Al_6O_{12}N_2$[4] and it is currently the most widely accepted. This formula indicates a 60 eq% Al content. The second formula is $Si_2Al_3O_7N$[7] and represents 52·9 eq% Al. The third formula is $Si_{12}Al_{18}O_{39}N_8$[3] and also indicates an eq% Al of 52·9.

X-phase sialon was also reported[5] to be present in the production of $\beta'$-sialon ($z = 3$) through simultaneous carbothermal reduction and nitridation of kaolinite at 1450°C, after about 1 h holding time. However, the phase disappeared after about 4 h. Considering that kaolinite is $2SiO_2 . Al_2O_3 . 2H_2O$, which would indicate an eq% Al of 42·9, and that so far, the various positions of X-phase on the $Si_3N_4$–AlN–$SiO_2$–$Al_2O_3$ diagram are between 53 and 60 eq% Al, the behaviour of X-phase mentioned above could be assumed to be consistent with two or three phase regions of Fig. 1. Thus, its presence in $\beta'$-sialon formation could be considered transitory but, surprisingly, Kokmeijer *et al.*,[8] using the same carbothermal route as above[5] to produce $\beta'$-sialon ($z = 3$) with the same process parameters and about the same amount of carbon, did not observe any X-phase.

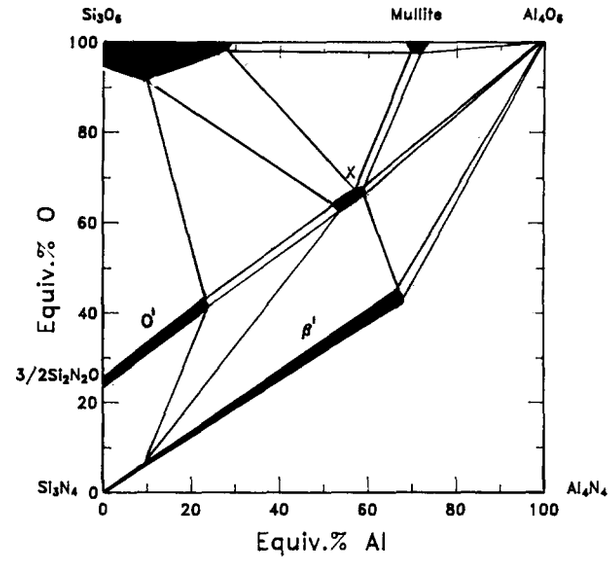


**Fig. 1.** Part of the $Si_3N_4$–AlN–$Al_2O_3$–$SiO_2$ system.[6]

$$\text{Eq\% Al} = \frac{[\text{Al}]/3}{[\text{Si}]/4 + [\text{Al}]/3} \cdot 100$$

where [Al] and [Si] represent the number of atoms of each of these elements present in the formula. 3 and 4 are the valencies of aluminium and silicon respectively.

It is reported[4] that X-phase sialon exists in two crystallographic forms—low and high—and that it is characterized by planar defects.[2,4] These planar defects complicate[2] the diffraction intensities. Although there seems to be a general consensus on the structure of the low form of X-phase, which is of a triclinic structure, the lattice parameters differ amongst the reports and even within individual reports (Table 1). This difference was attributed[4] to a

**Table 1.** Suggested crystal structures of X-phase sialon found in the literature

| *Number* | *Crystal structure* | *a (Å)* | *b (Å)* | *c (Å)* | *α (°)* | *β (°)* | *γ (°)* | *Reference* |
|---|---|---|---|---|---|---|---|---|
| 1 | Triclinic (low x) | 9·68 | 8·56 | 11·21 | 90 | 124·4 | 98·5 | 4 |
| 2 | Triclinic[a] (high x) | 9·66 | 2·84 | 11·17 | 90 | 124·4 | 98·5 | 4 |
| 3 | Triclinic | 9·9 | 9·7 | 9·5 | 109 | 95 | 95 | 10 |
| 4 | Triclinic | 8·56 | 9·85 | 9·69 | 70 | 81 | 81 | 1 |
| 5 | Triclinic | 11·21 | 9·69 | 8·56 | 99 | 90 | 124 ± 0·5 | 1, 2 |
| 6 | Orthorhombic | 7·85 | 9·12 | 7·965 | — | — | — | 11 |
| 7 | Monoclinic | 9·728 | 8·404 | 9·572 | — | 108·96 | — | 6 |

[a] It was suggested[9] that the most convenient representation of high X-phase is obtained using a pseudo-orthorhombic body-centred cell.

varied choice of cell by the authors. On the other hand, high X-phase was also reported[4] to have a triclinic structure (Table 1) but most conveniently represented[9] using a pseudo-orthorhombic cell.

So far reports on the properties of X-phase sialon are very limited. However, one of the reports[12] found in the literature relating to the mechanical properties of a composite of $\beta'$-sialon ($z = 3{\cdot}4$) and an unspecified amount of X-phase, suggested that the presence of X-phase in $\beta'$-sialons is detrimental to the mechanical properties of the latter. These data are scanty and therefore may not present a balanced assessment of the mechanical properties of X-phase. For a further mechanical property characterization of this phase, it is necessary that pure X-phase is produced. The uncertain nature of the chemistry of this phase, as reviewed in the preceding paragraphs, could make it difficult for a pure X-phase to be produced in a large quantity. However, a better understanding of its stoichiometry and structure will reduce this difficulty.

The present work is part of a wider programme to produce ceramic components containing X-phase by a carbothermal nitridation process from natural oxides. This is seen as an economic means of producing these materials.

## 2 Review of Reaction Mechanisms Based on the Three Formulae of X-Phase

### 2.1 Kaolinite + carbon mixture

For stoichiometric calculations, it is necessary to adopt the closest representative formula for X-phase. Equations for the formation from kaolinite of X-phase of the three formulae discussed above are, respectively,

$$3(2SiO_2 \cdot Al_2O_3 \cdot 2H_2O) + 3C + N_2 \xrightarrow{1500°C} Si_3Al_6O_{12}N_2 + 3SiO_2 + 3CO + 6H_2O \quad (1)$$

$$3(2SiO_2 \cdot Al_2O_3 \cdot 2H_2O) + 3C + N_2 \xrightarrow{1500°C} 2(Si_2Al_3O_7N) + 2SiO_2 + 3CO + 6H_2O \quad (2)$$

$$9(2SiO_2 \cdot Al_2O_3 \cdot 2H_2O) + 12C + 4N_2 \xrightarrow{1500°C} Si_{12}Al_{18}O_{39}N_8 + 6SiO_2 + 12CO + 18H_2O \quad (3)$$

Thus, the stoichiometric amounts of carbon required for X-phase and silica formation at 1500°C are 4·4, 4·4 and 5·8 wt%, respectively, for eqns (1) to (3).

However, a pre-stage to the formation of X-phase is the transformation of kaolinite to mullite ($3Al_2O_3 \cdot 2SiO_2$) according to eqn (4).

$$3(2SiO_2 \cdot Al_2O_3 2H_2O) \longrightarrow (3Al_2O_3 \cdot 2SiO_2) + 4SiO_2 + 6H_2O \quad (4)$$

The reaction in eqn (4) occurs at about 1200°C and the (amorphous) silica may be further converted to SiO in the presence of carbon according to equation:

$$SiO_2 + C \leftrightarrows SiO + CO \quad (5)$$

Alternatively, SiO may react with nitrogen and carbon to form $Si_3N_4$ according to eqn (6):

$$3SiO + 2N_2 + 3C \rightarrow Si_3N_4 + 3CO \quad (6)$$

Hence, the silica in eqn (4) would require some carbon for transformation to $Si_3N_4$. Therefore, depending on how much of the formed silica transforms to SiO or $Si_3N_4$ and the X-phase stoichiometry adopted, various minimum amounts of total carbon, greater than those indicated by stoichiometric eqns (1) to (3), would be required if X-phase, with or without excess silica, is to be formed.

### 2.2 Kaolinite + α-alumina + carbon mixture

From Fig. 1[6] and other reports[3-5] that represent X-phase as a point composition, irrespective of the formula adopted, it is clear that α-alumina must be mixed with kaolinite, if single-phase X-phase is to be formed by a carbothermal reduction route. Thus, using the formula $Si_3Al_6O_{12}N_2$,[4] general equations for its formation are

$$3(2SiO_2 \cdot Al_2O_3 \cdot 2H_2O) + 3Al_2O_3 + 6C + 2N_2 \xrightarrow{1500°C} 2(Si_3Al_6O_{12}N_2) + 6CO + 6H_2O \quad (7)$$

or

$$2(2SiO_2 \cdot Al_2O_3 \cdot 2H_2O) + Al_2O_3 + 3C + N_2 \xrightarrow{1500°C} (Si_3Al_6O_{12}N_2) + SiO_2 + 3CO + 4H_2O \quad (8)$$

Equation (7), stoichiometrically, would need 28·3 wt% (50 mol%) alumina, as a proportion of alumina and kaolinite only and 6·3 wt% C, relative to the solid reactants. However, the equation does not require excess silica to balance the Si/Al ratio as in the case of kaolinite alone. In other words, there is an absence of glass in the form of amorphous silica as a co-product of the transformation. On the other hand, eqn (8), with different stoichiometry, requires $SiO_2$ to balance the Si/Al ratio and would need 16·5 wt% (33 mol%) α-alumina, as a proportion of alumina and kaolinite and about 5·5 wt% C of the total solid reactants. Thus, the amount of carbon required depends on the stoichiometry adopted.

The stoichiometric equation for the formation of X-phase of formula $Si_2Al_3O_7N$[7] at 1500°C is:

$$2(2SiO_2 \cdot Al_2O_3 \cdot 2H_2O) + Al_2O_3 + 3C + N_2 \xrightarrow{1500°C} 2(Si_{12}Al_3O_7N) + 3CO + 4H_2O \quad (9)$$

Thus, the conditions for balancing eqn (9) are identical to those of eqn (8).

From a mixture of kaolinite, alumina and carbon, X-phase of formula $Si_{12}Al_{18}O_{39}N_8$ would be formed according to equation:

$$8(2SiO_2 . Al_2O_3 . 2H_2O) + Al_2O_3 + 12C + 4N_2 \xrightarrow{1500°C} Si_{12}Al_{18}O_{39}N_8 + 4SiO_2 + 12CO + 16H_2O \quad (10)$$

Stoichiometrically, eqn (10) implies that 6·2 wt% C, relative to the total weight of solid reactants, and 4·7 wt% α-alumina, as a proportion of kaolinite and alumina only, would be needed to produce X-phase.

## 3 Adoption of Reference Contents of Carbon and Alumina in Green Mixtures for Experiments

Equations (1) to (3) and (7) to (10) imply that five stoichiometric values (4·4, 5·8, 6·3, 5·5 and 6·2 wt%) of carbon content in green mixtures can lead to the formation of X-phase, with or without excess silica. Also, eqns (7) to (10) indicate three values (28·3, 16·5 and 4·7 wt%) of α-alumina content that can lead to the formation of X-phase. Hence, it is necessary to rationalize which of the values is most consistent for the formation of a stable monocrystalline product of X-phase.

For this purpose, some preliminary experiments were carried out, and the first observation of the experiments was that $Si_3N_4$ whiskers were formed at about 1300°C, thus justifying the need for extra carbon to be added to the stoichiometric amount of carbon required for X-phase formation.

A second observation was that a higher carbon content, limited by the appearance of $\beta'$, according to Fig. 1, is required if the formed x-phase is to be stable. The implication is that for each case of the mixtures (kaolinite–carbon and kaolinite–carbon–alumina), equations (formulae) that indicate a higher value of carbon requirement should be closest in representing the system. A corollary to this is that any representative formula should have a relatively low oxygen/nitrogen (O/N) ratio (oxygen content). Hence, based on the O/N-ratio factor of the three formulae and taking into consideration the two observations from the preliminary experiments, a nominal amount of carbon, greater than those stoichiometrically indicated by equations with the formula $Si_{12}Al_{18}O_{39}N_8$ was adopted as the carbon requirement for pre-stage transformations and X-phase formation only. However, it was reported[5] that carbon is lost by oxidation during heating to reaction temperatures and a compensation for such a loss was, therefore, also made in determining the final adopted carbon level for the process.

Since the adopted reference total carbon requirement relates to $Si_{12}Al_{18}O_{39}N_8$ and, since, according to eqn (10), X-phase formation from the kaolinite–carbon–alumina mixture is associated with 4·7 wt% alumina content, 5 wt% alumina, as a proportion of alumina and kaolinite only, was adopted as the reference alumina content of this mixture. The adopted reference carbon level is taken as 6 wt%. Three other mixtures different to the reference ones were made; two for the kaolinite–carbon mixture, with an extra 0·5 and 1 wt%, respectively, added to the adopted carbon level, while the third for the kaolinite–carbon–alumina mixture, with 4 wt% alumina. These mixtures are shown in Table 2.

**Table 2.** Composition of different green mixtures used in this study

| *Batch no.* | $C^a$ (*wt%*) | $Al_2O_3{}^b$ | | *Kaolinite*[b] | |
|---|---|---|---|---|---|
| | | (*wt%*) | (*mol%*)[c] | (*wt%*) | (*mol%*)[c] |
| 1 | 6 | — | — | 94 | — |
| 2 | 6·5 | — | — | 93·5 | — |
| 3 | 7 | — | — | 93 | — |
| 4 | 6 | 5 | 11·7 | 95 | 88·3 |
| 5 | 6 | 4 | 9·5 | 96 | 90·5 |

[a] The carbon content is related to the entire green mixture.
[b] The alumina and kaolinite contents are related to the sum of their partial concentrations considered as 100%.
[c] Mol% is deduced from the wt% (w) by using the molecular weight ($M$) of the component thus:

$$\text{mol}_i\% = \frac{\frac{W_i}{M_i}}{\sum_{i=1}^{n} \frac{W_i}{M_i}} 100$$

where $n$ is the number of components.

## 4 Experimental Procedure

The kaolinite used in this work was supplied by EEC International plc (Cornwall, UK) and is of grade D. The activated carbon was supplied by the Aldrich Chemical Company (ACC) Ltd (Dorset, UK), while the α-alumina (corundum) was supplied by the Morganite Thermal Company (MTC) Ltd (Stourport-on-Severn, Worcestershire, UK). The chemical analyses of these raw materials are given in Table 3.

The powders, as in Table 2, were mixed with propan-2-ol and milled with alumina balls overnight. The green mixture was dried overnight and then broken manually to 2·6 ± 0·7 mm granules.

A vertical mullite tube furnace of 38 mm internal diameter heated by a silicon carbide spiral element was used. The granules were introduced into a

**Table 3.** Compositions of raw materials

| *ECC (grade D) clay* (*wt%*) | | *ACC activated carbon* (*wt%*) | | *MTC alumina (961)* (*wt%*) | |
|---|---|---|---|---|---|
| $SiO_2$ | 46·88 | Ash | 3 | $Al_2O_3$ | 98·3 |
| $Al_2O_3$ | 37·65 | Extractable phosphates | 0·5 | $SiO_2$ | 0·7 |
| $Fe_2O_3$ | 0·88 | | | $Fe_2O_3$ | 0·2 |
| $TiO_2$ | 0·09 | | | MgO/CaO | 0·2 |
| CaO | 0·03 | | | $Na_2O/K_2O$ | 0·4 |
| MgO | 0·13 | | | | |
| $K_2O$ | 1·60 | | | | |
| $Na_2O$ | 0·21 | | | | |
| Loss on ignition | 12·45 | | | | |
| Mineralogical constitution (%) | | | | | |
| Kaolinite | 85 | | | | |
| Mica | 12 | | | | |
| Feldspar | 3 | | | | |

cylindrical graphite crucible (with a grid of 1-mm holes at the base) to a height of 35 mm. With the furnace hot zone at the reaction temperature of $1500 \pm 5$°C, the crucible was introduced to the hot zone within about 25 min. The advancement of the charge to the hot zone was carried out by moving upwards a closed-end mullite sheath, in which there was a Pt/Pt–13% Rh thermocouple and on which the crucible was sitting. The actual temperature of the charge at any point in time was measured with this thermocouple.

The nitrogen flow rate was controlled by a capillary flow meter, and a volume flow rate of about 1·61 litre $min^{-1}$ (linear flow rate of about 141 cm $min^{-1}$) was used.

The charge was evacuated by moving the thermocouple sheath downwards and the average cooling rate was about 55° $min^{-1}$.

Examination of the end products was carried out using X-ray (Guinier camera with Cu$K_\alpha$ radiation) and electron microscopy (transmission (TEM), Philips EM 400T and scanning (SEM), Philips PSEM 500)/EDAX techniques. With the aid of a computer program, the observed interplanar distances from the XRD pattern were used to determine the lattice parameters of the formed phase. For TEM, the powder was ground with chloroform and a suspension of this was deposited on a holey carbon film supported by a copper grid. KCl was used for determining the camera constant. Hence, both the KCl standard and the specimens were always observed under the same conditions of voltage (100 kv), magnification and specimen height.

## 5 Results and Discussions

In Table 4 are the observed and calculated X-ray data of low X-phase found in the present work. For interplanar spacings with more than two sets of Miller indices, only two are entered in the table. The lattice parameters obtained are $a = 9{\cdot}68$ Å, $b = 8{\cdot}55$ Å, $c = 11{\cdot}21$ Å, $\alpha = 91{\cdot}4°$, $\beta = 124{\cdot}4°$ and $\gamma = 99{\cdot}2°$, corresponding to a triclinic structure. This set of parameters is similar to that suggested by Thompson & Korgul[4] for low X-phase (Table 1).

About 96% X-phase with 4% mullite (visual estimation) crystalline phases were observed after 5 h of heating batch 1 (Table 2) at 1500°C. To test the stability of the X-phase, this charge was further heated for 13·5 h at the same temperature in a nitrogen atmosphere. The composition remained the same (Fig. 2(a)(i)). Therefore the disappearance of the phase in the work of Higgins & Hendry[5] could be attributable to the amount of carbon used for $\beta'$-sialon formation being beyond that required for X-phase formation and X-phase being produced in varying mixtures.

Batches 2 and 3 in Table 2 were treated under the same heating conditions as above for 5 h, with a view to the extra carbon leading to a further transformation of the remaining 4% mullite to X-phase. The result was that essentially pure X-phase was formed, with a trace of mullite remaining and a trace of $\beta'$-sialon nucleated (Fig. 2(a) (ii) and (iii)).

For batch 4, under the same heating conditions and within 5 h, X-phase was the principal crystalline product, a trace of mullite remained and up to 10% $\alpha$-alumina was produced (Fig. 2(b)(i)—again an indication that the monophase domain of X-phase had been passed.

Batch 5 gave principally X-phase with a small amount of $\beta'$-sialon and mullite after heating for 5 h (Fig. 2(b)(ii)), but on heating for a further 13 h, $\alpha$-alumina was copiously formed (Fig. 2(b)(ii)), with a reduction in the amount of mullite.

In all the batches, there was always a trace of

**Table 4.** Observed and calculated X-ray data for low X-phase[a] found in the present work

| (*hkl*) | *Interplanar spacing, d (Å)* | | *Observed intensity*[b] |
|---|---|---|---|
| | *Observed* | *Calculated* | |
| $10\bar{1}$ | 9·054 | 9·056 | vvw |
| 010 | 8·412 | 8·414 | vvw |
| 100 | 7·856 | 7·862 | s |
| $1\bar{1}0$ | 6·342 | 6·338 | vw |
| 011 | 5·918 | 5·916 | w |
| $10\bar{2}$ | 5·608 | 5·606 | ms |
| 110 | 5·292 | 5·292 | vvw |
| $20\bar{1}$ | 4·715 | 4·717 | w |
| $21\bar{1}$ | 4·434 | 4·433 | mw |
| $01\bar{2}$ | 4·224 | 4·223 | w |
| 020 | 4·207 | 4·207 | w |
| $02\bar{1}$, $12\bar{1}$ | 3·982 | 3·984, 3·979 | w |
| 200 | 3·932 | 3·931 | w |
| 012 | 3·874 | 3·874 | vw |
| $21\bar{2}$ | 3·822 | 3·823 | vw |
| $10\bar{3}$ | 3·649 | 3·650 | s |
| $20\bar{3}$ | 3·619 | 3·622 | vs |
| 120 | 3·460 | 3·461 | vw |
| $12\bar{1}$ | 3·442 | 3·447 | w |
| $12\bar{2}$ | 3·364 | 3·361 | w |
| 210 | 3·343 | 3·340 | vw |
| $02\bar{2}$, $21\bar{3}$ | 3·274 | 3·277, 3·275 | vw |
| $22\bar{2}$ | 3·257 | 3·258 | vw |
| $31\bar{2}$ | 3·141 | 3·142 | vvw |
| 201 | 3·041 | 3·041 | mw |
| $30\bar{1}$ | 3·016 | 3·015 | mw |
| $01\bar{3}$ | 2·984 | 2·982 | vvw |
| $22\bar{2}$ | 2·932 | 2·932 | vw |
| $20\bar{4}$ | 2·801 | 2·803 | ms |
| $32\bar{2}$ | 2·746 | 2·745 | vw |
| $10\bar{4}$ | 2·653 | 2·654 | w |
| 300 | 2·620 | 2·621 | ms |
| 130 | 2·502 | 2·504 | s |
| 103 | 2·425 | 2·427 | vw |
| 202 | 2·390 | 2·390 | w |
| $22\bar{4}$ | 2·331 | 2·330 | vvw |
| $12\bar{4}$ | 2·308 | 2·306 | vvw |
| $01\bar{4}$, $23\bar{2}$ | 2·282 | 2·280, 2·279 | ms |
| $23\bar{3}$, $40\bar{4}$ | 2·263 | 2·267, 2·264 | ms |
| $33\bar{1}$, $23\bar{1}$ | 2·257 | 2·256 | vvw |
| $20\bar{5}$ | 2·225 | 2·225 | w |
| 301 | 2·209 | 2·210 | mw |
| $03\bar{3}$, $41\bar{2}$ | 2·182 | 2·184, 2·182 | mw |
| $10\bar{5}$ | 2·074 | 2·074 | w |
| $40\bar{5}$ | 2·046 | 2·047 | vw |
| $24\bar{0}$ | 2·009 | 2·010 | w |
| 203, 024 | 1·937 | 1·940, 1·937 | vvw |
| 104 | 1·931 | 1·931 | vw |
| 231 | 1·906 | 1·905 | w |
| $33\bar{1}$, $14\bar{2}$ | 1·896 | 1·896 | w |
| $03\bar{4}$, $13\bar{4}$ | 1·875 | 1·874 | vvw |
| $30\bar{6}$ | 1·869 | 1·869 | vvw |
| $33\bar{4}$, $43\bar{4}$ | 1·860 | 1·860 | vvw |
| $50\bar{2}$ | 1·844 | 1·845 | vvw |
| $04\bar{3}$ | 1·824 | 1·824 | vw |
| $50\bar{5}$, $40\bar{6}$ | 1·811 | 1·811 | vw |
| $23\bar{5}$ | 1·763 | 1·763 | vw |
| $32\bar{6}$, $53\bar{3}$ | 1·706 | 1·706 | vw |
| 232 | 1·689 | 1·689 | w |
| 420, $51\bar{6}$ | 1·670 | 1·670 | w |
| $52\bar{3}$, $34\bar{3}$ | 1·647 | 1·647 | vvw |
| $03\bar{5}$ | 1·617 | 1·617 | vvw |
| $34\bar{4}$, $22\bar{4}$ | 1·594 | 1·594 | w |
| $33\bar{6}$, $43\bar{6}$ | 1·553 | 1·553 | w |
| $24\bar{3}$ | 1·549 | 1·549 | w |
| $52\bar{1}$, $34\bar{5}$ | 1·503 | 1·503 | w |

[a] Triclinic structure, having $a = 9{\cdot}68$ Å, $b = 8{\cdot}55$ Å, $c = 11{\cdot}21$ Å, $\alpha = 91{\cdot}4°$, $\beta = 124{\cdot}4°$ and $\gamma = 99{\cdot}2°$.
[b] s = strong; m = medium; mw = medium weak; w = weak; vw = very weak; vvw = very very weak.

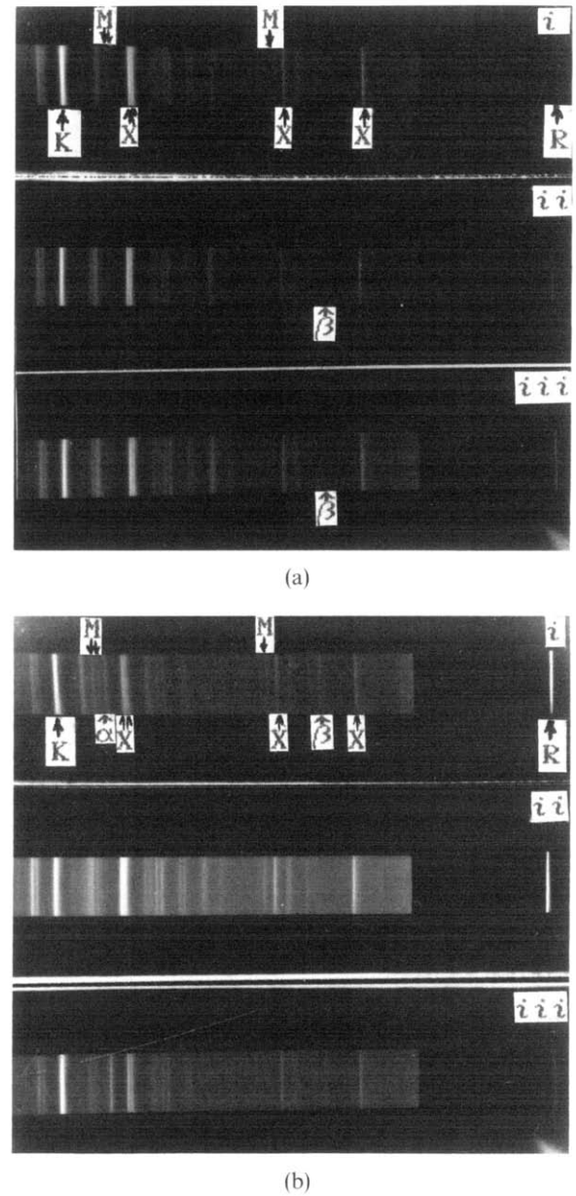


**Fig. 2.** Low-angle section of XRD patterns of end products of (a) green mixtures without alumina: (i) batch 1, 18·5 h; (ii) batch 2, 5 h; (iii) batch 3, 5 h; (b) green mixtures with alumina: (i) batch 4, 5 h; (ii) batch 5, 5 h; (iii) batch 5, 18 h. Only the principal lines of the phases are indicated. $\alpha = \alpha$-Alumina, $\beta = \beta'$-sialon, M = mullite, K = KCl, R = reference line and X = X-phase.

mullite. Since batch 5 within 5 h also showed a trace of $\beta'$-sialon, it could be that with 4 wt% (9·5 mol%) alumina the amount of carbon in the green mixture needed to be slightly reduced, if only crystalline X-phase (with negligible trace of mullite) were to be formed. Hence, it could be inferred that the domains of existence of X-phase extend toward higher oxygen (lower nitrogen) contents, from 42·9 eq%Al (representing the vertical of kaolinite composition) towards the $SiO_2$–$Al_2O_3$ line of the $Si_3N_4$–AlN–$SiO_2$–$Al_2O_3$ equilibrium diagram (similar to that proposed by Jack[6] (Fig. 7).

The formation of α-alumina with 5 wt% (11 mol%) alumina suggests that a composition or formula marked by this or greater amounts of alumina (eq% Al), is in error in representing a monophase domain of X-phase. Using samples of natural minerals of muscovite and kyanite as standards, further support to this statement was established from TEM EDAX analyses of 20 crystals of x-phase, in which an average value of $1{:}1{\cdot}5 \pm 0{\cdot}1$ for Si/Al ratio was obtained. Hence this domain extends from 42·9 to less than 49·6 eq% Al.

Since the formula $Si_{12}Al_{18}O_{39}N_8$ has the nearest eq% Al value to 49·6, it is the closest representative amongst the formulae proposed so far. Although $Si_2Al_3O_7N$ also has the same eq% Al, as already discussed above, its O/N ratio is not consistent with the carbon level calculations. In addition, $Si_2Al_3O_7N$ does not permit the balancing of Si/Al ratios with excess amorphous silica (glass) when X-phase is formed by mixing kaolinite and alumina. However, SEM EDAX results of bulk products of the run showed peaks of silicon higher than those of aluminium, indicating that a second phase containing silicon was also present.

Figure 3 shows one in a series of the EDAX results obtained from the end products of batch 1. The quantitative relationship of component elements of a material is given as:[10]

$$\frac{C_A}{C_B} = K_{AB}\frac{I_A}{I_B} \quad \text{(Ref. 13)} \qquad (11)$$

where A and B represent respective elements, $C$ is their individual concentration in the material, $I$ is their spectral energy or intensity from EDAX spectrum and $K_{AB}$ is a coefficient, which for Al–Si, from different studies,[13] varies from 1·12 to 1·42. In this study, however, using the natural minerals mentioned above, $K_{AB}$ was found to be $1{\cdot}05 \pm 0{\cdot}05$. If both Si/Al ratios of 1:1·5 (indicated by $Si_{12}Al_{18}O_{39}N_8$ and $Si_2Al_3O_7N$) and 1:2 (indicated by $Si_3Al_6O_{12}N_2$), and the various $K_{AB}$ values are substituted into eqn (11), it can be seen that there is always an excess of silicon. The silicon content of mullite is lower than that of aluminium, so this excess silicon can not be due to the presence of trace mullite. This excess must, therefore, be due to the presence of an additional phase that has a substantial amount of silicon. Thus, equations which do not require excess $SiO_2$ for balancing Si/Al ratios do not truly represent the system.

The co-precipitation of the three crystalline phases—mullite, X-phase and β′—should not be possible, according to Fig. 1. Thus, the fact that the three were actually present when the carbon content of the mixture is increased by 0·5 wt% can only be due to micro-heterogeneity and the restricted area which marks the monophase domain of X-phase.

Although the X-ray data revealed the phase to be of low X-form with a triclinic structure, the ED patterns of the phase could not be indexed as a triclinic structure. However, on assuming an orthorhombic (pseudo-orthorhombic[9]) structure and em-

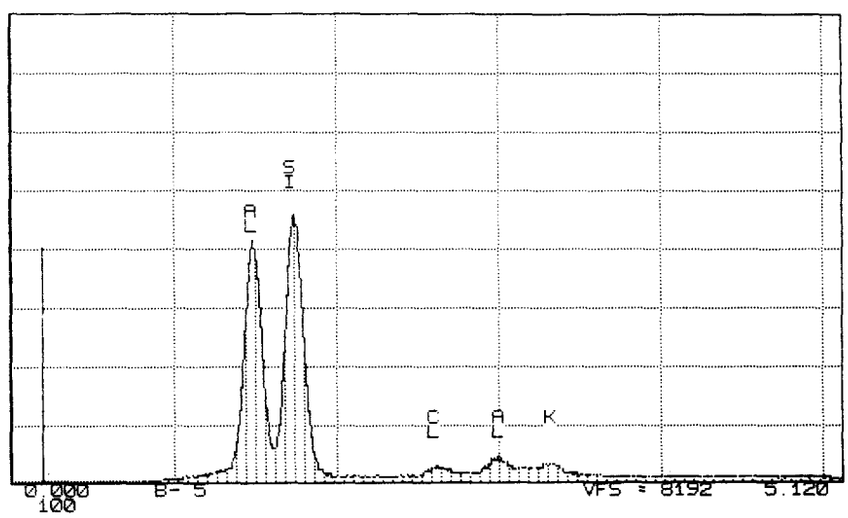


QUALITATIVE ELEMENT IDENTIFICATION

SAMPLE ID:

POSSIBLE IDENTIFICATION
SI KA
AL KA & SUM PEAK
CL KA
K KA OR IN LA?
FE KA

PEAK LISTING

| | ENERGY | AREA | EL. AND LINE |
|---|---|---|---|
| 1 | 1.476 | 49533 | AL KA |
| 2 | 1.744 | 57883 | SI KA |
| 3 | 2.618 | 2406 | CL KA |
| 4 | 2.979 | 3563 | AL SUM |
| 5 | 3.309 | 2246 | K KA OR IN LA? |
| 6 | 6.401 | 896 | FE KA |

**Fig. 3.** SEM EDAX spectra of end products of batch 1.

**Table 5.** Indexing parameters of X-phase from TEM studies[a]

| *Number* | *Remarks* | $d_1d_2$ (°) | $d_1d_3$ (°) | $d_1$ (Å) | $d_2$ (Å) | $d_3$ (Å) |
|---|---|---|---|---|---|---|
| | Observed | 82 | 41 | 3·72 | 3·72 | 2·45 |
| 1 | Calculated | 81·7 | 40·8 | 3·67 | 3·67 | 2·42 |
| | (*hkl*) | | | 202 | $20\bar{2}$ | 400 |
| | Observed | 91 | 48·5 | 2·14 | 2·07 | 1·50 |
| 2 | Calculated | 92 | 47 | 2·18 | 2·11 | 1·50 |
| | (*hkl*) | | | $10\bar{5}$ | $3\bar{1}1$ | $4\bar{1}4$ |
| | Observed | 90 | 48 | 2·80 | 2·53 | 1·89 |
| 3 | Calculated | 90 | 48·5 | 2·80 | 2·48 | 1·86 |
| | (*hkl*) | | | 004 | 210 | 214 |
| | Observed | 108 | 73 | 2·15 | 1·33 | 1·33 |
| 4 | Calculated | 108·4 | 72·8 | 2·18 | 1·33 | 1·33 |
| | (*hkl*) | | | 105 | $12\bar{3}$ | 222 |
| | Observed | 80 | 55 | 2·69 | 1·41 | 1·16 |
| 5 | Calculated | 80·7 | 55·2 | 2·69 | 1·41 | 1·18 |
| | (*hkl*) | | | 104 | 121 | 225 |
| | Observed | 50 | 28 | 2·65 | 2·21 | 1·33 |
| 6 | Calculated | 50·5 | 27·8 | 2·69 | 2·22 | 1·35 |
| | (*hkl*) | | | 104 | 402 | 506 |
| | Observed | 90 | 51 | 1·95 | 1·56 | 1·22 |
| 7 | Calculated | 90 | 51·6 | 1·95 | 1·55 | 1·21 |
| | (*hkl*) | | | 114 | $60\bar{2}$ | 712 |
| | Observed | 40 | 25 | 7·35 | 4·92 | 3·15 |
| 8 | Calculated | 40·8 | 24·8 | 7·33 | 4·85 | 3·10 |
| | (*hkl*) | | | 101 | 200 | 301 |

[a] Considered as orthorhombic, with a = 9·66 Å, b = 2·84 Å, c = 11·17 Å.

ploying the unit cell lengths (*a*, *b* and *c*) suggested for high X-phase by Thompson & Korgul,[4] (Table 1) all the patterns were consistently and accurately indexed (Table 5). The observed interplanar angles and distances, in all the cases, differed from the calculated values by $\leq \pm 1{\cdot}5°$ and $< \pm 1{\cdot}5\%$, respectively (Table 5). Figures 4 and 5 are examples of the X-phase. Note the faults in Figs 4(b) (dark field).

The ambiguity between results of XRD and ED of X-phase was also observed by Drew & Lewis.[10] The high *d*-spacings measured by the ED method in their work were not detected by XRD, and they attributed this to a probable superlattice nature of X-phase. They also noted that their proposed lattice parameters and triclinic structure were not consistent for all of the reflections supposed to belong to the phase observed in the TEM.

Zangvil[1] observed X-phase in the TEM of a triclinic structure, with $a = 8{\cdot}56$ Å, $b = 9{\cdot}85$ Å, $c = 9{\cdot}69$ Å, $\alpha = 70°$, $\beta = 81°$ and $\gamma = 81 \pm 0{\cdot}5°$. However, in the same work[1] and confirmed in a later work,[2] a new set of parameters are proposed, which obviously can no longer be used to index the x-phase observed[1] in the TEM.

Low X-phase is considered to be a superlattice of high X-phase, and it is most conveniently represented by the [010] projection using the pseudo-orthorhombic body-centred cell[4] (hence the assumption in this work of an orthorhombic structure). From the consistency of the indexing, there can be no doubt that in the TEM X-phase is observed which can be indexed with an orthorhombic (pseudo-orthorhombic) structure.

It was suggested[14] that reflections from plate-like structures in ED are better than those of XRD in characterizing individual polymorphic modifications and the order or disorder within a complete structure. Therefore, the discrepancy between the XRD and ED observations in this study possibly lies in the differences between the two techniques. Hence, whereas XRD investigations are averaged over the whole volume of the material, which is in constant rotation and therefore is independent of a preferred orientation of individual crystals, results of ED analyses are dependent on the orientation of the crystal, relative to the beam direction. For instance, although the ED patterns were obtained from different angles of tilt and rotation of a crystal and different crystals, most of the zone axes (*uvw*) of the patterns in Table 5 showed a particular trend of *v* being positive and greater than *u* and *w* coordinates. In most case, they could be reduced to [010], for example, the sets of planes in numbers 1, 6 and 7 of Table 5 which all give zone axes of [010].

Thus, ED patterns reveal the specific nature and features of crystals that make up the structure. So, it could be that in ED the orientation of plate-structured crystals of x-phase is such that only the

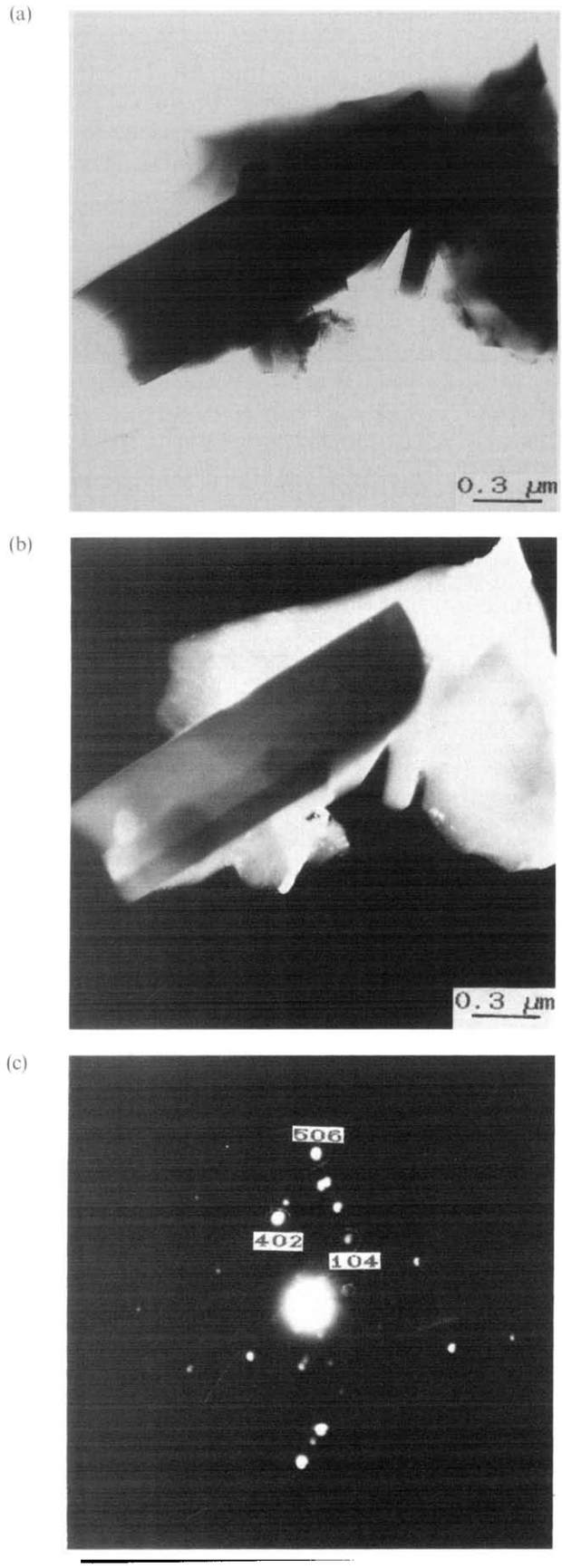


**Fig. 4.** X-phase sialon: (a) bright field; (b) dark field; (c) diffraction pattern, entered in Table 5 as number 6. Note the faults in the dark field.

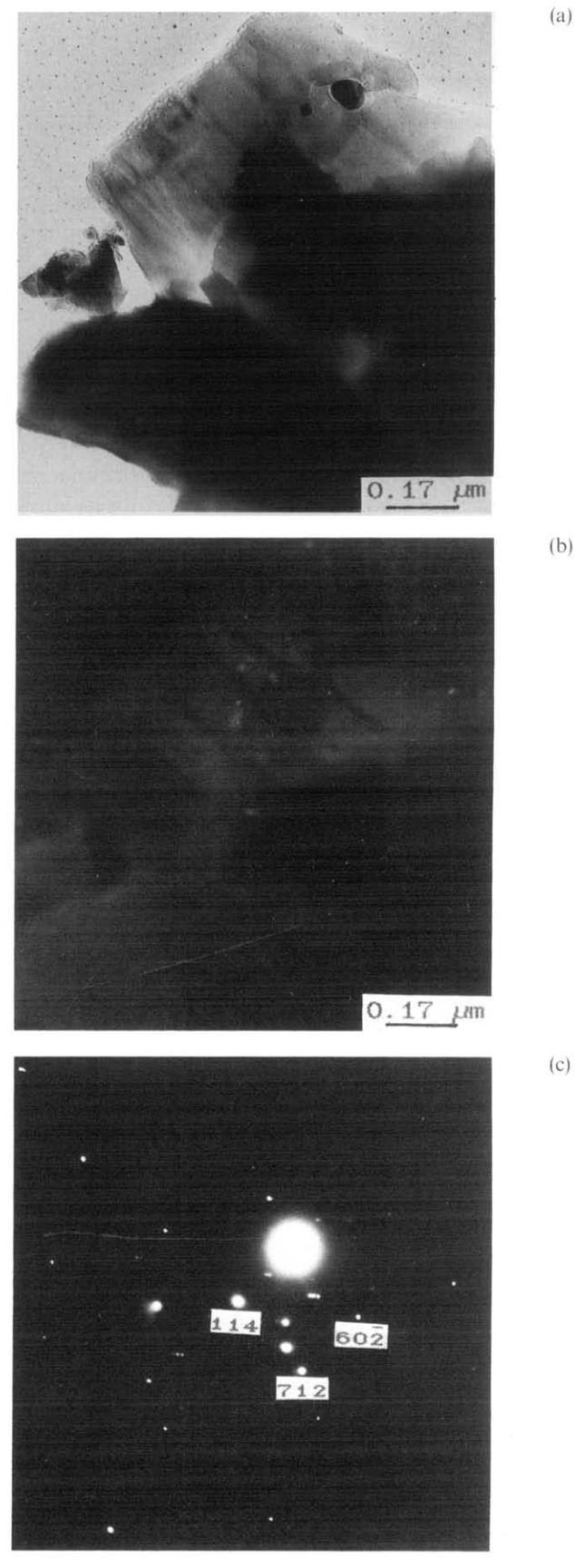


**Fig. 5.** X-phase sialon: (a) bright field; (b) dark field; (c) diffraction pattern, entered in Table 5 as number 7. Faults are visible in the dark field.

orthorhombic (pseudo-orthorhombic) symmetry is favoured.

## 6 Conclusions

Stable X-phase is formable by simultaneous carbothermal reduction and nitridation route.

Of the three published formulae for X-phase sialon, $Si_{12}Al_{18}O_{39}N_8$ is suggested to be the closest representative. In a paper published subsequent to the present work being completed, Bergman *et al.*[15] reported experiments to establish phase equilibria in the Si–Al–O–N system at 1700–1775°C. A limited number of samples in phase fields containing X-phase were prepared by pressureless sintering or hot isostatic pressing and a formula of $Si_{12}Al_{18}O_{36}N_{10}$ was shown to give the most reliable composition from EDS analysis for pressureless sintered samples. HIPed samples, however, gave similar Si and Al coefficients but a higher oxygen content than in pressureless sintering. Bergman *et al.* conclude therefore that there is a range of composition for X-phase. The present results are consistent with those of Bergman *et al.* in the Si:Al ratio and together support the formula proposed by Naik *et al.*[3] with a restricted range of solid solubility. The domain of the phase is so narrow that stringent process control may be required to ensure a minimal presence of impurities such as mullite and/or $\beta'$-sialon and/or $\alpha$-alumina.

The low X-form is triclinic in structure and this is observable as such in XRD. In the TEM, diffraction patterns are indexed as orthorhombic. This discrepancy is probably due to preferred orientation usually associated with ED studies. Thus the orientation to the beam direction of individual crystals under investigation is always such that orthorhombic (pseudo-orthorhombic) symmetry is favoured.

## Acknowledgement

Financial support under the BRITE-EURAM programme (contract number Breu-0064-EDB) is acknowledged. The authors are grateful to Dr J. Engell and Mr C. Daugaard, both of the Technical University, Lyngby, Denmark for access to the computer program used for generating X-ray lattice parameters.

## References

1. Zangvil, A., *J. Mat. Sci. Lett.*, **13** (1978) 1370.
2. Zangvil, A., Gauckler, L. J. & Ruhle, M., *J. Mat. Sci. Lett.*, **15** (1980) 788.
3. Naik, I. K., Gauckler, L. J. & Tien, T. Y., *J. Amer. Cer. Soc.*, **61**(7/8) (1978) 332.
4. Thompson, D. P. & Korgul, P., In *2nd NATO ASI Conf. Proc. Progress in Nitrogen Ceramics*, ed. F. L. Riley. M. Nijhoff, 1983, p. 375.
5. Higgins, I. & Hendry, A., *Brit. Cer. Trans. J.*, **85** (1986) 161.
6. Jack, K. H., *J. Mat. Sci.*, **11** (1976) 1135.
7. Rae, A. W. J. M., Thompson, D. P. & Jack, K. H., In *Ceramics for High Performance Applications, II*, ed. J. J. Burke *et al.* Brookhill, Massachusetts, 1978, p. 1039.
8. Kokmeijer, E., Scholte, C., Blomer, F. & Meteselaar, R., *J. Mat. Sci.*, **25** (1990) 1261.
9. Thompson, D. P., In *Preparation and Properties of Silicon Nitride-based Materials*, ed. D. A. Bonnell & T. Y. Tien. Publ. Trans. Tech., Switzerland, 1989, p. 21.
10. Drew, P. & Lewis, M. H., *J. Mat. Sci.*, **9** (1974) 1833.
11. Gugel, E., Petzenhauser, I. & Fickel, A., *Powder Met. Int.*, **7** (1975) 66.
12. Wills, R. R., Stewart, R. W. & Wimmer, J. M., *Cer. Bull.*, **56**(2) (1977) 194.
13. Williams, D. B., *Practical Analytical Electron Microscopy in Mats. Sci.* Verlag Chemie International, Basel, Florida, 1984, p. 67.
14. Zvyagin, B. B., *Electron Diffraction Analysis of Clay Mineral Structures*. Plenum Press, New York, 1967, p. 67 (translated from Russian by Simon Lyse).
15. Bergman, B., Ekstrom, T. & Micski, A., *J. Eur. Cer. Soc.*, **8** (1991) 141.